

Experimental Studies on Multiphase Flow in Porous Media and Pore Wettability

Xingxun Li, and Xianfeng Fan

Abstract—Multiphase flow transport in porous medium is very common and significant in science and engineering applications. For example, in CO₂ Storage and Enhanced Oil Recovery processes, CO₂ has to be delivered to the pore spaces in reservoirs and aquifers. CO₂ storage and enhance oil recovery are actually displacement processes, in which oil or water is displaced by CO₂. This displacement is controlled by pore size, chemical and physical properties of pore surfaces and fluids, and also pore wettability. In this study, a technique was developed to measure the pressure profile for driving gas/liquid to displace water in pores. Through this pressure profile, the impact of pore size on the multiphase flow transport and displacement can be analyzed. The other rig developed can be used to measure the static and dynamic pore wettability and investigate the effects of pore size, surface tension, viscosity and chemical structure of liquids on pore wettability.

Keywords—Enhanced oil recovery; Multiphase flow; Pore size; Pore wettability;

I. INTRODUCTION

THREE-phase flow transport in porous media is relevant to many problems of great scientific and industrial importance, such as extraction of oil, gas and geothermal energy from underground reservoirs, CO₂ storage and transport of contaminants in soils and aquifers [1]. Even though significant progress has been made, many challenges are still remaining. For example, almost 70% of oil from underground still cannot be recovered, because the oil is held in porous media. In CO₂ storage and enhanced oil recovery, CO₂ must be delivered to the place, not only large geological cracks, but also pore space. Pore space contributes to 60% of CO₂ geological storage capacity[2]. The transport of CO₂ in the confined space is governed by liquid composition, liquid viscosity, capillary forces, the physical and chemical properties of liquids and pore surfaces, pore structure, saturation of pores etc [3]. Most of these factors are interrelated. For example, the impact of liquid viscosity and liquid surface tension on CO₂ transport varies greatly with pore size, pore structure, the physical and chemical properties of pore surfaces, and pore wettability [4]. The wetting phenomenon of fluids within porous medium has been intensively investigated for oil/gas recovery from reservoir rocks and for soil science [5]. The pore wettability characterized by a contact angle formed by the intersection of

the interfaces connecting the three phase [6] plays a significant role in multiphase transports and fluid displacements in pores [7]-[9]. Due to lack of the technique for measuring the contact angle in small pores and the common assumption of the external flat surface representing the internal surface of pore [10], the pore contact angle has been simply estimated by either using the contact angle measured on a flat surface by a sessile drop experiment [11]-[14] or oversimplified and simply treated as zero for complete wetting case [15], [16] which may be true in some cases but deserves to be checked and criticized[17], [18], or indirect measurements, such as a capillary rise technique, a liquid intrusion calorimetry, a thin-layer wicking technique, and distance-time and weight-time imbibition techniques based on Laplace equation and Lucas-Washburn equation [17]-[22]. All these previous work for evaluation of the wettability in porous media were plausible but needs to be further studied and confirmed. So, it is important and necessary to measure and study the contact angle at pores to indicate the pore wettability correctly and avoid misusing improper contact angles for porous surface case.

II. EXPERIMENTAL

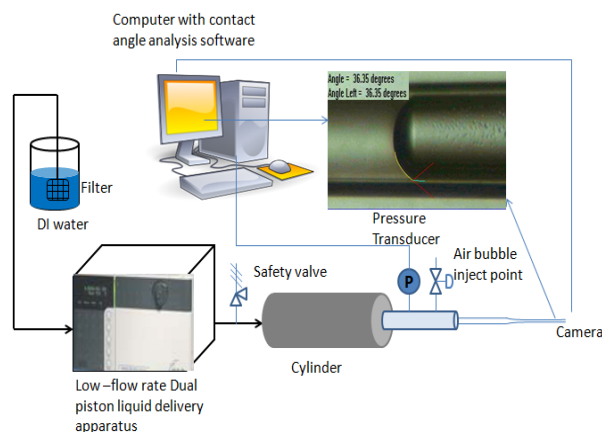


Fig. 1 Multiphase flow transport experimental setup

The rig illustrated in Fig.1 is for measuring the pressure profile for driving a two-phase flow through a capillary tube to study the transport of multiphase flow in a single pore. The rig includes five parts: a solution resource providing constant fluid stream, a pump which delivers solution from resources, a cylinder which is filled solutions, a pressure transducer and a digital camera recording resistance pressure and movement of two-phase flow respectively. The capillary tubes with a diameter from 75 μ m and 600 μ m were made from clean glass

Xingxun Li is with the School of Engineering, The University of Edinburgh, Edinburgh, EH9 3JL, UK (phone: +44(0)131 06505685; fax: +44(0)131 6506551; e-mail: X.Li@ed.ac.uk).

Xianfeng Fan, is with the School of Engineering, The University of Edinburgh, Edinburgh, EH9 3JL, UK (phone: +44(0)131 6506551; fax: +44(0)131 6506551; e-mail: X.Fan@ed.ac.uk).

tubes through heating and stretching. The length of stretched glass capillary is fixed at 1---1.5 cm. The DI water was first pumped to capillaries by a Solvent Delivery Unit (LC-2AD, Shimadzu) at a flowrate of 0.01 ml/min. After the water flow reached a constant flowrate, the air-water interfaces flew through the capillary. The pressure for driving the fluids was measured by a pressure transducer with a resolution of 0.1 mbar (DPI 280, Druck).

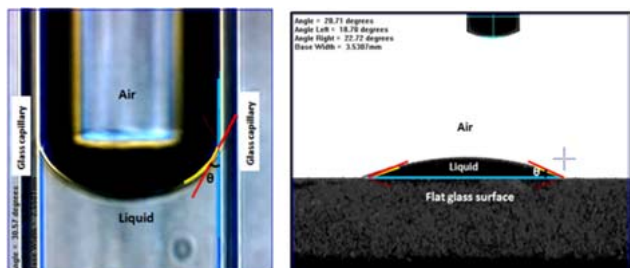


Fig. 2 Measurement and analysis of pore contact angles and contact angles on a flat surface

For pore wettability studies, the capillary tubes with a diameter from 20 μ m to 1000 μ m were made from highly cleaned glass tubes. The experiments were started by placing a single capillary onto a clean glass slide support. The central of the capillary was focused by a digital camera (AM7023 Dino-Eye). The capillary flow and the interface of invading liquid front were observed and imaged under the high-resolution digital camera. When any dynamic movement of liquid was completely stopped and the equilibrium status of liquid in a capillary was reached, the image of meniscus can be taken and analyzed by our contact angle analysis software (First Ten Angstroms, FAT 32) to obtain the static contact angle (Fig. 2 (left)). The static contact angle of a liquid on a flat surface was measured by the sessile drop method (Fig.2 (right)). Five typical kinds of liquids (distilled water, 1-propanol, n-decane, crude oil and silicone oil) with various surface tensions, viscosities and chemical structures were used.

III. RESULTS AND DISCUSSION

Fig. 3 presents the pressure profile for driving an air-water two phase flow through a capillary tube. In Fig. 3, section 0-A includes two stages, which are air bubble compression and fluid flow acceleration. The pressure inside the channel increases progressively. At point A, the force applied to the air-water flow is balanced with the resistance from the capillary and viscous resistance. In section A-B, the air-water interface does not enter the capillary, the measured pressure is for driving water phase through the capillary. At point B, the air-water interface enters the capillary. From B to C, the air-water interface moves through the capillary. The measured pressure rises sharply. The section BC can also be seen as the displacement of water by air in the capillary. The measured pressure will be called displacement pressure in this study. At the peak point C, the two-phase interface comes out from the capillary and pressure drops drastically and returns to the

pressure value in section A-B. At the point D, air is completely out of the tube. The section DE is for the movement of single-phase water in the capillary, and the pressure reaches equilibrium for the single water phase. The interesting phenomenon observed from this measurement is that the resistance pressure to air-water interface is significantly larger than the pressure to a single phase. This means that the displacement of liquid by a gas requires a pressure significantly higher than the pressure for driving a single phase. The air bubble deformation and two-phase interface in the capillary become significant for the displacement pressure profile. However, in practice, the resistance pressure from a single phase of a fluid is always used to estimate the displacement processes.

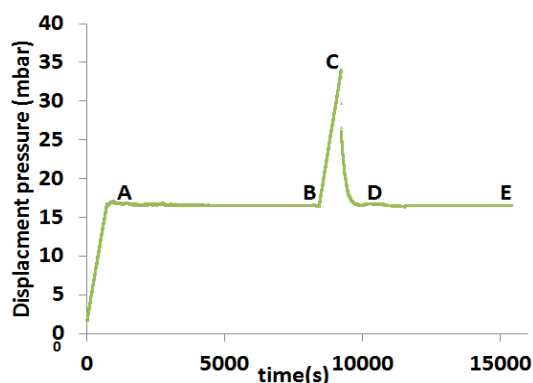


Fig. 3 Displacement pressure profile for a capillary with a size of 180 μ m at 0.01 ml/min driving flow rate

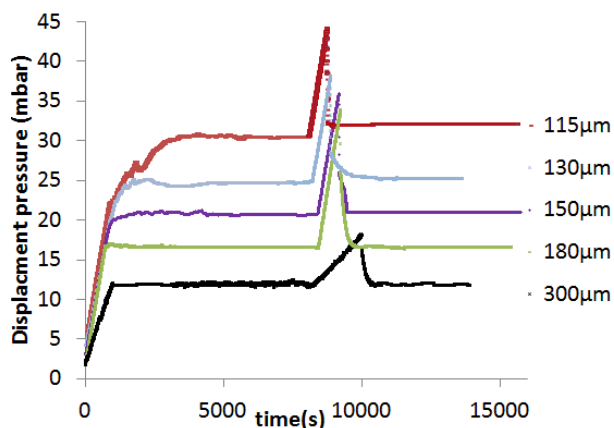


Fig. 4 Pressure profile for water displacement by air in capillaries with various sizes (115 μ m, 130 μ m, 150 μ m, 180 μ m and 300 μ m) at 0.01 ml/min driving flow rate

The results in Fig. 4 and 5 show that capillary size has a significant impact on a single phase flow and the air-water displacement. As shown in Fig. 4, the larger capillary gives the smaller balance pressure to both water flow and air-water interface in glass tubes before the air-water interface going into capillary tubes. During the air-water interface passing the capillary, the results clearly show the air-water displacement pressure for a smaller capillary is always larger than that from

the capillary with a larger size. The relationship between the displacement pressure and capillary size is plotted in Fig. 5. The results indicate that the displacement pressure for air-water interface does not vary linearly with the capillary size. When the capillary size decreases from 600 μm to 200 μm , the pressure increases by 1000 Pa. However, the displacement pressure increases significantly by 2240 Pa with the decrease in capillary size from 200 μm to 70 μm .

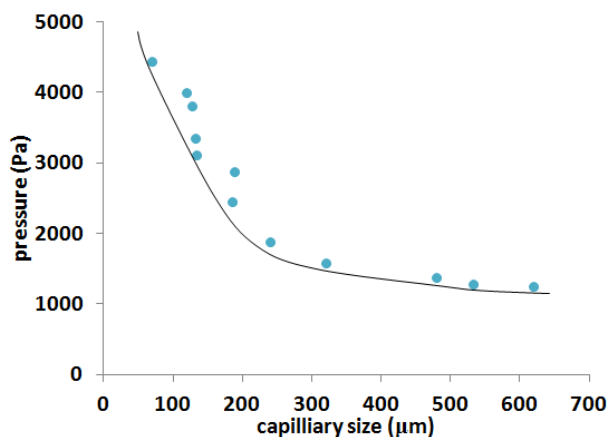


Fig. 5 Air-water displacement pressure against capillary size

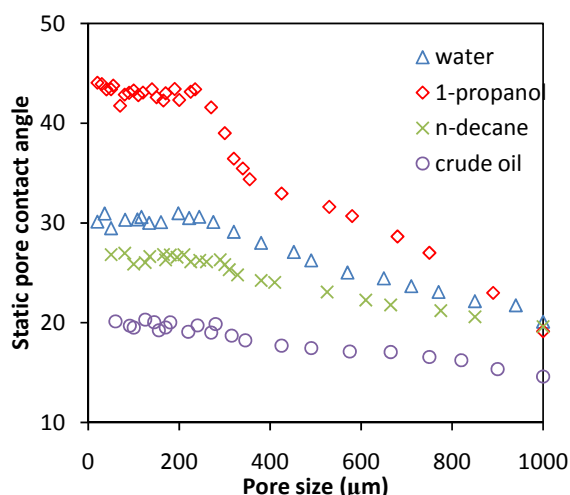


Fig. 6 Static pore contact angles for DI water, 1-propanol, n-decane and crude oil in glass capillaries with a size of 50 μm -1000 μm

To study the pore wettability, the static pore contact angles of water, 1-propanol, n-decane and crude oil in the range of capillary size from 50 μm to 1000 μm were measured by our new developed rig, which largely differs from the simplified theoretical assumption of $\theta = \theta_0$ (Fig.6). Fig.6 presents that the static pore contact angle varies with pore size. The static pore contact angle increases dramatically from the pore size of 1000 μm to 300 μm . When the pore size is roughly between 300 μm and 50 μm , the change of pore contact angle with pore size is not remarkable and the average static pore contact angles for these four liquids are 42.97 $^\circ$, 30.22 $^\circ$, 26.20 $^\circ$ and 19.69 $^\circ$,

respectively. The results in Fig.6 also indicate that the 1-propanol and water always give larger pore contact angles than those from n-decane and crude oil. The 1-propanol and crude oil have the largest and smallest variations of static pore contact angles with the pore size from 1000 μm to 50 μm , respectively.

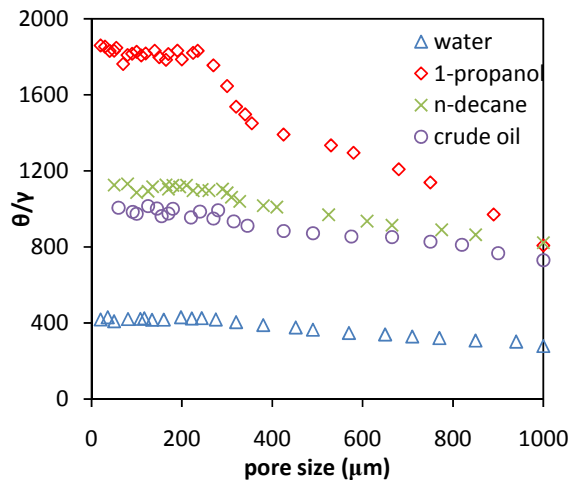


Fig. 7 Pore static contact angles at unit surface tension (θ/γ) for water, 1-propanol, n-decane and crude oil

Fig. 7 shows the pore static contact angle at unit surface tension (θ/γ) of each liquid. It could be used to estimate the effect of chemical structure of liquid on the pore contact angles due to eliminating the influence of surface tension. From the Fig.7, the contribution of unit surface tension of water (θ/γ) to its pore contact angle is the lowest among these four liquids, while the contribution of unit surface tension of 1-propanol (θ/γ) is the largest. In comparison of the chemical structure of the four chemicals, 1-propanol has two completely different parts in a molecule, one end (-OH) is strongly hydrophilic, another end is carbon chain, which is strongly hydrophobic. The highest contribution to the static contact angle may be due to their two extreme ends. n-decane and the crude oil give a similar (θ/γ) value because of their similar chemical structures and properties. Lack of -OH groups in the carbon chains of the n-decane and crude oil may lead to the lower (θ/γ) than that from 1-propanol. The chemical structure of liquid consequently has a significant effect on the pore contact angle or pore wettability.

The static contact angles for DI water, 1-propanol, n-decane and crude oil were also measured on flat glass surfaces and then compared with their pore contact angles (Fig. 8) correspondingly. It can be seen that the static contact angles on flat glass surfaces are smaller than those in pores for all these four kinds of liquids in Fig.8. The difference between contact angles in pores and on a flat glass surface increases with pore size decrease. The magnitude of the difference varies with the liquids, or their chemical structure. The largest difference is about 40 $^\circ$, from 1-propanol. Another interesting phenomenon is that the pore contact angle tends to draw close to its contact

angle on a flat surface when the pore size is big enough. The equal point of the two contact angles varies with the liquids. For water, the equal point is at the pore size of $1000\mu\text{m}$. Overall, the contact angle varies not only with pore size, but also with the physical and chemical properties of liquids, the surface tension, viscosity. It is very complex. We will investigate this problem in our future studies.

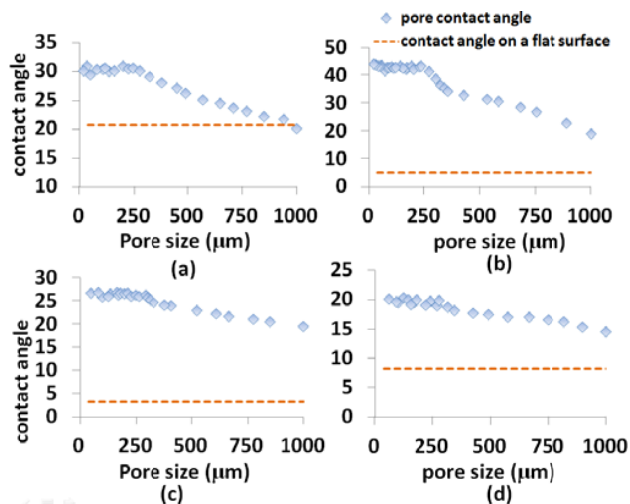


Fig. 8 Comparison of pore contact angles with contact angles on a flat surface. (a) DI water, (b) 1-propanol, (c) n-decane, (d) crude oil

Many investigators have only emphasized on the static contact angles (advancing or receding) regardless of the practical importance of dynamic wetting [6], [23]-[27]. Since the contact angle is always assumed to keep equilibrium all the time in the classic description of capillary rise by the Lucas-Washburn equation [28],[29], it has recently revived the interest in the dynamics of capillary flow [15] and questioned in the dependence of dynamic contact angle on the velocity of the three-phase contact line (TPCL) [30]-[34]. Therefore, in this study, the dynamic pore contact angles of water, 1-propanol, n-decane and crude oil in glass capillaries were also measured and shown in Fig.9 to indicate the dependence of dynamic pore contact angle on velocity and the effects of physical and chemical properties on dynamic pore wettability. Fig.9 shows that the dynamic pore contact angle monotonically increases with imbibition rate. It can be clearly seen that the dynamic pore contact angle of silicone oil and crude oil is highly velocity-dependent, while the dynamic pore contact angle profiles of water, 1-propanol and n-decane are less velocity-dependent. When the imbibition rate was from 0 to $1.2 \times 10^{-3} \text{m/s}$, the dynamic pore contact angles of water, 1-propanol and n-decane varied only by 3-5. 2. By contrast, the dependences of dynamic pore contact angles of crude oil and silicone oil on imbibition rate are much more remarkable due to their larger viscosities. The effect of surface tension on dynamic pore contact angle can be investigated by the dynamic pore contact angles of water and 1-propanol. Water and 1-propanol have close viscosities but very different surface tensions. Fig.9 shows that the dynamic pore contact angle of

1-propanol with a lower surface tension of 24.4mN/m varies with the imbibition rate by 5. 2, whereas the water with a higher surface tension of 72mN/m gives a lower variation in dynamic pore contact angle, only by 3. So, it can be concluded that a low liquid-gas surface tension tends to favor the variation of dynamic pore contact angle with imbibition rate and the liquid with higher viscosity has a more significant effect on the dynamic pore wettability alteration. However, the dynamic wetting behavior of crude oil is very different from the silicone oil. The crude oil has a viscosity of 8.3cst and a surface tension of 20mN/m , which are very close to the silicone oil with a viscosity of 10cst and a surface tension of 19.4mN/m , but the dynamic pore contact angles of crude oil are much higher and increased with the imbibition rate faster than those from the silicone oil (10cst). This means that the dynamic pore contact angle not only depends on liquid surface tension and liquid viscosity, but also depends on the chemical structure of liquids.

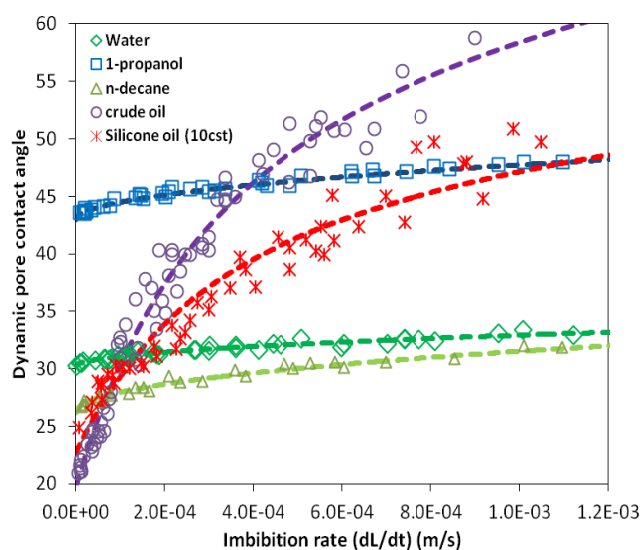


Fig. 9 Dependence of dynamic pore contact angle on velocity for water, 1-propanol, n-decane, crude oil and silicone oil

ACKNOWLEDGMENT

This work is supported by the Carnegie Trust for the Universities of Scotland, UK, and the Research Grant from the UK Royal Society (e-gap). We also would like to thank the technique support from Mr Gardiner Hill, the Director of Technology at BP, Dr Stephen J Cawley at BP, and Dr Jinhai Yang and Heron from the Edinburgh Heriot-Watt University.

REFERENCES

- [1] Y.-W. Yang, G. Zografis, and E. E. Miller, "Capillary flow phenomena and wettability in porous media: I. Static characteristics," *Journal of Colloid and Interface Science*, vol. 122, pp. 24-34, 1988.
- [2] J. Bear, "Dynamics of Fluids in Porous Media," *Dover Publications*, 1972
- [3] R. H. Brooks and A. T. Corey, *Hydraulic properties of porous media*. State University Colorado State University Hydrology Paper 3. Fort Collins, CO, 1964.

- [4] E. Aker and K. K. Ma^loy, "Simulating temporal evolution of pressure in two-phase flow in porous media," *Phys. Rev. E*, vol. 58, pp. 2217-2226, 1998.
- [5] J. F. Padday, *Wetting, Spreading and Adhesion*. New York: Academic Press, 1978.
- [6] M. Latva-Kokko and D. H. Rothman, "Static contact angle in lattice Boltzmann models of immiscible fluids," *Physical Review E*, vol. 72, p. 046701, 2005.
- [7] P. S. Laplace, Ed., "*Theory of Capillary Attraction*," *Supplements to the 10th book of "Celestial Mechanics" (1806, 1807), translated and annotated by N. Bowditch (1893)* Reprinted by Chelsea, New York, 1966). Paris, 1806, p. pp. Pages.
- [8] T. Young, "An Essay on the Cohesion of Fluids," *Phil. Trans. Roy. Soc. Lond.*, vol. 95, pp. 65-87, 1805.
- [9] J. E. Seebergh and J. C. Berg, "Dynamic wetting in the low capillary number regime," *Chemical Engineering Science*, vol. 47, pp. 4455-4464, 1992.
- [10] D. Patro, S. Bhattacharyya, and V. Jayaram, "Flow Kinetics in Porous Ceramics: Understanding with Non-Uniform Capillary Models," *Journal of the American Ceramic Society*, vol. 90, pp. 3040-3046, 2007.
- [11] W. G. Anderson, "Wettability literature survey. Part 2: Wettability measurement.," *JPT (Nov. 1986)*, vol. 38, pp. 1246-1262, 1986.
- [12] J. S. Buckley, "Mechanisms and consequences of wettability alteration by crude oils.," Heriot-Watt University PhD Thesis, Edinburgh, Scotland, 1996.
- [13] N. R. Morrow, "Wettability and its effect on oil recovery," *JPT (Dec. 1990)*, pp. 1476-1484, 1990.
- [14] D. Y. Kwok, R. Lin, M. Mui, and A. W. Neumann, "Low-rate dynamic and static contact angles and the determination of solid surface tensions," *Colloids and Surfaces A: Physicochemical and Engineering Aspects*, vol. 116, pp. 63-77, 1996.
- [15] M. N. Popescu, J. Ralston, and R. Sedev, "Capillary Rise with Velocity-Dependent Dynamic Contact Angle," *Langmuir*, vol. 24, pp. 12710-12716, 2008/11/04 2008.
- [16] A. Siebold, M. Nardin, J. Schultz, A. Walliser, and M. Oppliger, "Effect of dynamic contact angle on capillary rise phenomena," *Colloids and Surfaces A: Physicochemical and Engineering Aspects*, vol. 161, pp. 81-87, 2000.
- [17] F. Gomez, R. Denoyel, and J. Rouquerol, "Determining the Contact Angle of a Nonwetting Liquid in Pores by Liquid Intrusion Calorimetry," *Langmuir*, vol. 16, pp. 4374-4379, 2000/05/01 2000.
- [18] H. T. Xue, Z. N. Fang, Y. Yang, J. P. Huang, and L. W. Zhou, "Contact angle determined by spontaneous dynamic capillary rises with hydrostatic effects: Experiment and theory," *Chemical Physics Letters*, vol. 432, pp. 326-330, 2006.
- [19] D. Y. Kwok, C. J. Budziak, and A. W. Neumann, "Measurements of Static and Low Rate Dynamic Contact Angles by Means of an Automated Capillary Rise Technique," *Journal of Colloid and Interface Science*, vol. 173, pp. 143-150, 1995.
- [20] E. Chibowski and L. Hoysz, "On the use of Washburn's equation for contact angle determination," *Journal of Adhesion Science and Technology*, vol. 11, pp. 1289-1301, 1997.
- [21] L. Galet, S. Patry, and J. Dodds, "Determination of the wettability of powders by the Washburn capillary rise method with bed preparation by a centrifugal packing technique," *Journal of Colloid and Interface Science*, vol. 346, pp. 470-475, 2010.
- [22] L. Labajos-Broncano, M. L. Gonzalez-Martin, J. M. Bruque, and C. M. Gonzalez-Garcia, "Comparison of the use of Washburn's equation in the distance-time and weight-time imbibition techniques," *Journal of Colloid and Interface Science*, vol. 233, pp. 356-360, 2001.
- [23] A. Ishakoglu and A. F. Baytas, "The influence of contact angle on capillary pressure-saturation relations in a porous medium including various liquids," *International Journal of Engineering Science*, vol. 43, pp. 744-755, 2005.
- [24] M. Elena Diaz, J. Fuentes, R. L. Cerro, and M. D. Savage, "An analytical solution for a partially wetting puddle and the location of the static contact angle," *Journal of Colloid and Interface Science*, vol. 348, pp. 232-239, 2010.
- [25] F. Lu, M. Li, Z. Xu, and Y. Zhang, "Study of static contact angle measurement method based on least squares fitting," in *2nd Annual Conference on Electrical and Control Engineering, ICECE 2011, September 16, 2011 - September 18, 2011*, Yichang, China, 2011, pp. 844-847.
- [26] G. E. Wang and J. J. Lannutti, "Static wetting of a liquid drop on a solid," *Journal of Materials Science*, vol. 30, pp. 3171-3176, 1995.
- [27] Z.-N. Xu, F.-C. Lu, H.-T. Zhang, and Y.-P. Liu, "Influencing factors of silicone rubber static contact angle measurement," *Gaodianya Jishu/High Voltage Engineering*, vol. 38, pp. 147-156, 2012.
- [28] R. Lucas, *Kolloid Z*, vol. 23, p. 15, 1918.
- [29] E. W. Washburn, *Phys. Rev.*, vol. 17, pp. 273-283, 1921.
- [30] T. D. Blake, in *wettability*, pp. 251-309, 1993.
- [31] R. L. Hoffman, *J. Colloid Interface Sci*, vol. 50, p. 228, 1974.
- [32] R. G. Cox, *J. Fluid Mech.*, vol. 168, p. 169, 1986.
- [33] T. D. Blake and J. M. Haynes, *J. Colloid Interface Sci*, vol. 30, p. 421, 1969.
- [34] Y. D. Shikhmurzaev, *Int. J. Multiphase Flow*, vol. 19, p. 589, 1993.